Table S1. Gd^{3+}–Gd^{3+} distances in MBP and T4 lysozyme mutants

		Gd^{3+}-Gd^{3+} distance/nm				
		MBP-A[a]		T4L-A[c]	T4L-B[d]	T4L-C[e]
		- maltose	+ maltose			
IDA-SH	experimental	3.8	3.8	3.9	4.2	
T1-Gd	experimental	3.7	3.8	4.2	4.2[g] 4.1[h]	3.9
	predicted	3.6	3.7	3.9	3.7	3.8
T2-Gd	experimental	3.6	3.7	4.2	4.2	3.9[g] 3.9[h]
	predicted	3.6	3.6	3.9	3.8	3.8
		MBP-B[b]			T4L-D[f]	
C9	experimental	4.0	3.9		4.0[g] 3.9[h]	
	predicted	3.9	4.0		4.3	

[a] MBP-A: quadruple mutant S233C/T237C/Y341C/T345C

[b] MBP-B: double mutant T237C/T345C

[c] T4L-A: mutant C54T/C97A/D72C/R76C/D127C/V131C

[d] T4L-B: mutant C54T/C97A/D72C/R76C/V131C/K135C

[e] T4L-C: mutant C54T/C97A/D72C/R76D/R80C/D127C/V131D/K135C

[f] T4L-D: mutant C54T/C97A/D72C/V131C

[g] from DEER experiment

[h] from RIDME experiment

Table S2. Experimental and predicted widths of DEER distance distributions produced by the Gd^{3+} tags attached to T4 lysozyme and MBP mutants

		full width at half height/nm				
		MBP-A[a]		T4L-A[c]	T4L-B[d]	T4L-C[e]
		- maltose	+ maltose			
IDA-SH	experimental	0.78	0.84	0.56	0.56	
T1-Gd	experimental	1.06	0.93	0.28	0.38[g] 0.38[h]	0.27
	predicted	0.56	0.48	0.30	0.30	0.22
T2-Gd	experimental	1.06	0.88	0.38	0.28	0.27[g] 0.25[h]
	predicted	0.56	0.56	0.30	0.28	0.24
		MBP-B[b]			T4L-D[f]	
C9	experimental	1.25	0.81		0.79[g] 0.49[h]	
	predicted	0.84	0.66		0.52	

[a] MBP-A: quadruple mutant S233C/T237C/Y341C/T345C

[b] MBP-B: double mutant T237C/T345C

[c] T4L-A: mutant C54T/C97A/D72C/R76C/D127C/V131C

[d] T4L-B: mutant C54T/C97A/D72C/R76C/V131C/K135C

[e] T4L-C: mutant C54T/C97A/D72C/R76D/R80C/D127C/V131D/K135C

[f] T4L-D: mutant C54T/C97A/D72C/V131C

[g] from DEER experiment

[h] from RIDME experiment

Table S3. Gd^{3+}–Gd^{3+} distances and widths of distance distributions produced by the **T1-Gd** and **T2-Gd** tags in the *i*,*i*+8 attachment mode

	T4 lysozyme mutant					
	T4L-C[a]		T4L-E[b]		T4L-F[c]	
	T1-Gd	**T2-Gd**	**T1-Gd**	**T2-Gd**	**T1-Gd**	**T2-Gd**
Gd^{3+}–Gd^{3+} distance/nm	3.9[d]	3.9[d]/3.9[e]	3.9[d]/3.8[e]	4.0[d]	4.1[d]/4.0[e]	4.1[d]
full width at half amplitude/nm	0.27[d]	0.27[d]/0.25[e]	0.60[d]/0.43[e]	0.70[d]	0.64[d]/0.44[e]	0.72[d]

[a] T4L-C: mutant C54T/C97A/D72C/R76D/R80C/D127C/V131D/K135C

[b] T4L-E: mutant C54T/C97A/D72C/R80C/D127C/K135C

[c] T4L-F: mutant C54T/C97A/D72C/R76D/R80C/D127C/K135C

[d] from DEER experiment

[e] from RIDME experiment

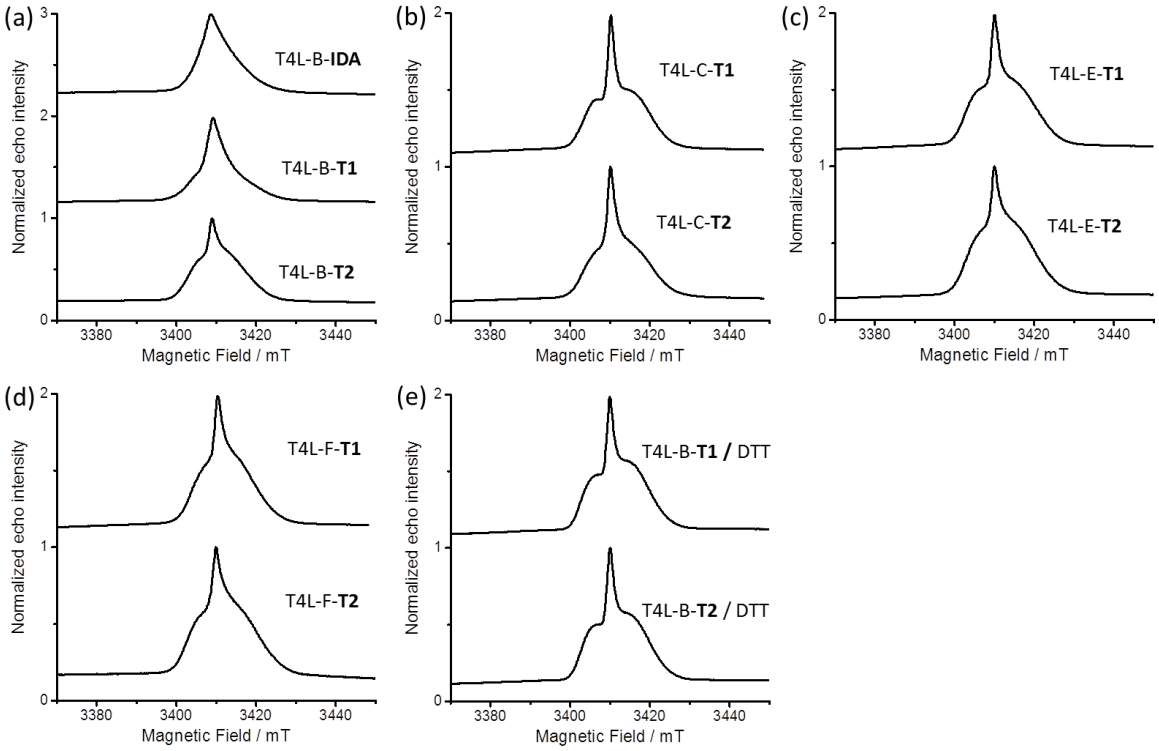

Figure S1. ED-EPR spectra of the region of the central transition region obtained for the **T1-Gd** and **T2-Gd** tags associated with the T4 lysozyme mutants (a) T4L-B, (b) T4L-C, (c) T4L-E, and (d) T4L-F. Panel (e) presents the spectra of the T4L-B mutants after treatment with 20 equivalents DTT at room temperature for 30 minutes before freezing and measurement, in order to reduce the S-S bond conjugation to the protein and release the tag. These spectra thus represent free tag and, as expected, are practically the same for the **T1-Gd** and **T2-Gd** tag. Comparison with the other panels shows that the spectral line shape of the tags is more or less conserved between free and bound tag, except for small differences that depend on the specific mutant and chirality of the tag. All spectra were normalized to unity and are shifted by 1 for improved visualization and comparison.

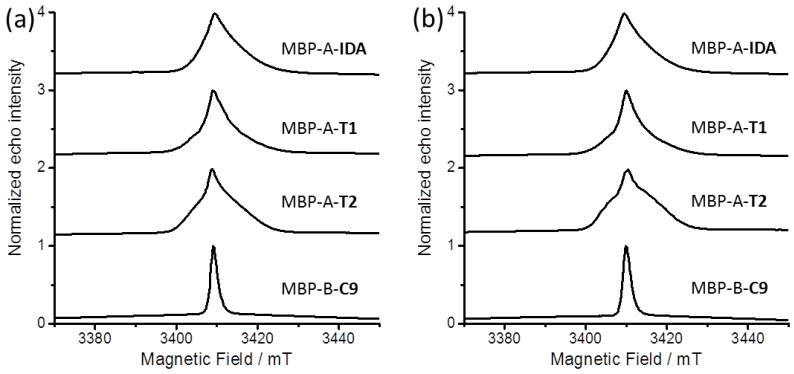

Figure S2. ED-EPR spectra of the region of the central transition obtained for the Gd^{3+} ions in different tags attached to the MBP mutants.

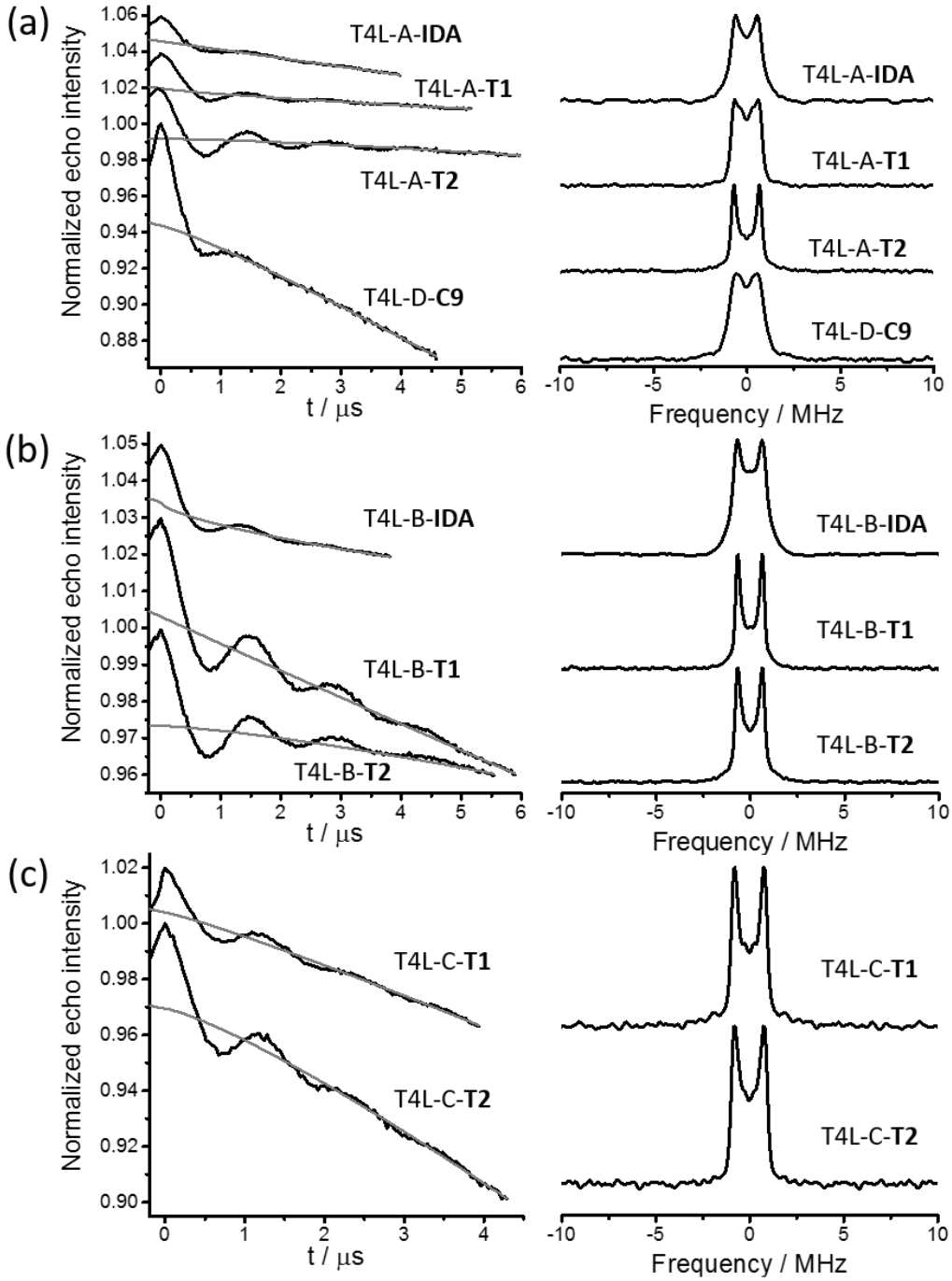

Figure S3. Primary DEER traces and Fourier transformed spectra obtained with different Gd^{3+} tags on T4 lysozyme mutants. (a) T4L-A and T4L-D. (b) T4L-B. (c) T4L-C. (Left) Primary DEER traces (black) and the background function used (grey). (Right) Corresponding data after background subtraction and Fourier transformation.

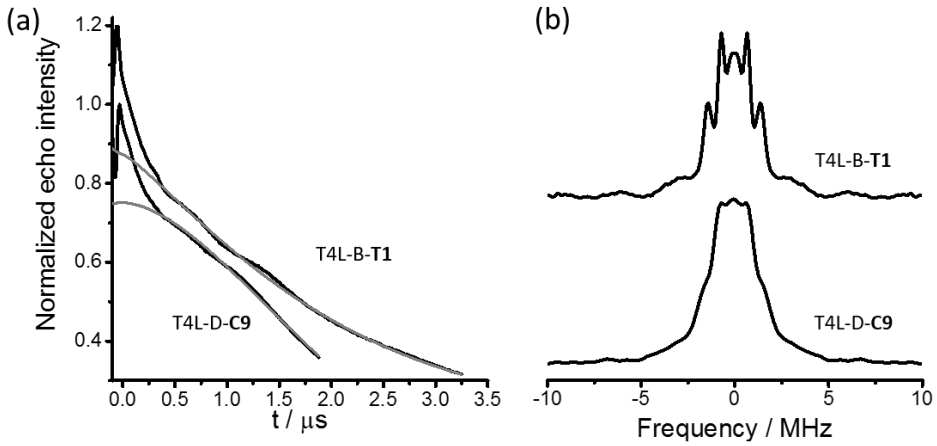

Figure S4. RIDME results of T4L-B-**T1** and T4L-D-**C9**. (a) Primary RIDME traces. The fitted background decays are indicated by grey lines. (b) Corresponding data after background subtraction and Fourier transformation.

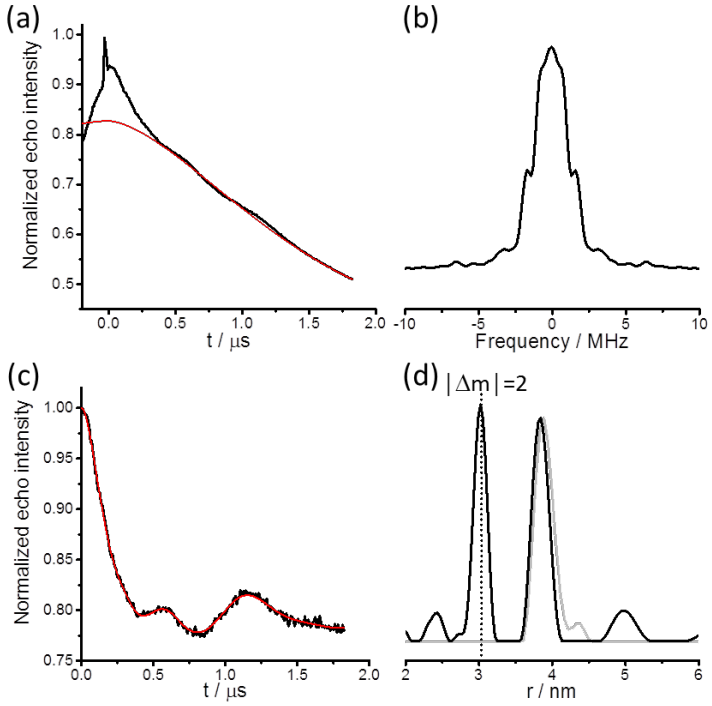

Figure S5. RIDME results of T4L-C-**T2**. (a) Primary data along with the background correction function used in red. (b) The Fourier transform of the experimental trace in (a). (c) Background corrected RIDME traces (black) along with the fit obtained with the distance distributions shown in (d) (red). (d) Comparison of the distance distributions obtained from the analysis of RIDME (black) and DEER (grey) data. The dotted line shows the position expected for the second harmonic calculated from the main peak.

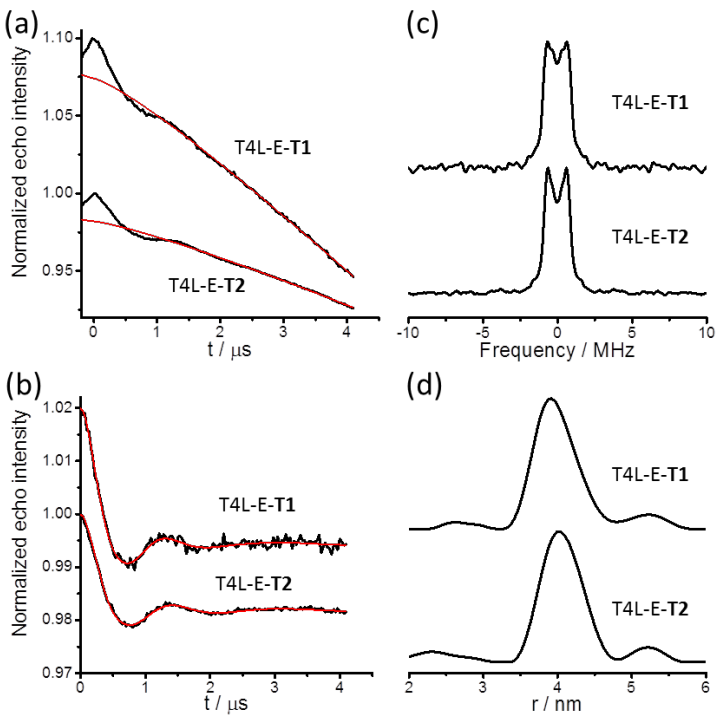

Figure S6. DEER results of T4L-E-**T1** and T4L-E-**T2**. (a) Primary data along with the background correction function used in red. (b) Background corrected DEER traces (black) along with the fit obtained with the distance distributions shown in (d) (red). (c) Fourier transform of the experimental traces in (b). (d) Distance distributions obtained from the analysis shown in (b).

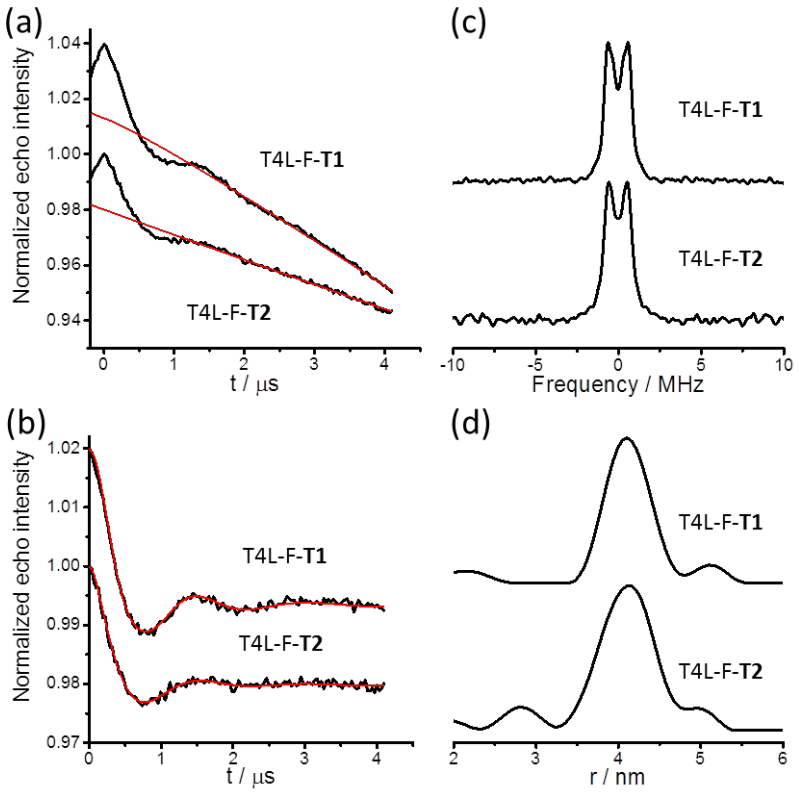

Figure S7. DEER results of T4L-F-**T1** and T4L-F-**T2**. (a) Primary data along with the background correction function used in red. (b) Background corrected DEER traces (black) along with the fit obtained with the distance distributions shown in (d) (red). (c) Fourier transform of the experimental traces in (b). (d) Distance distributions obtained from the analysis shown in (b).

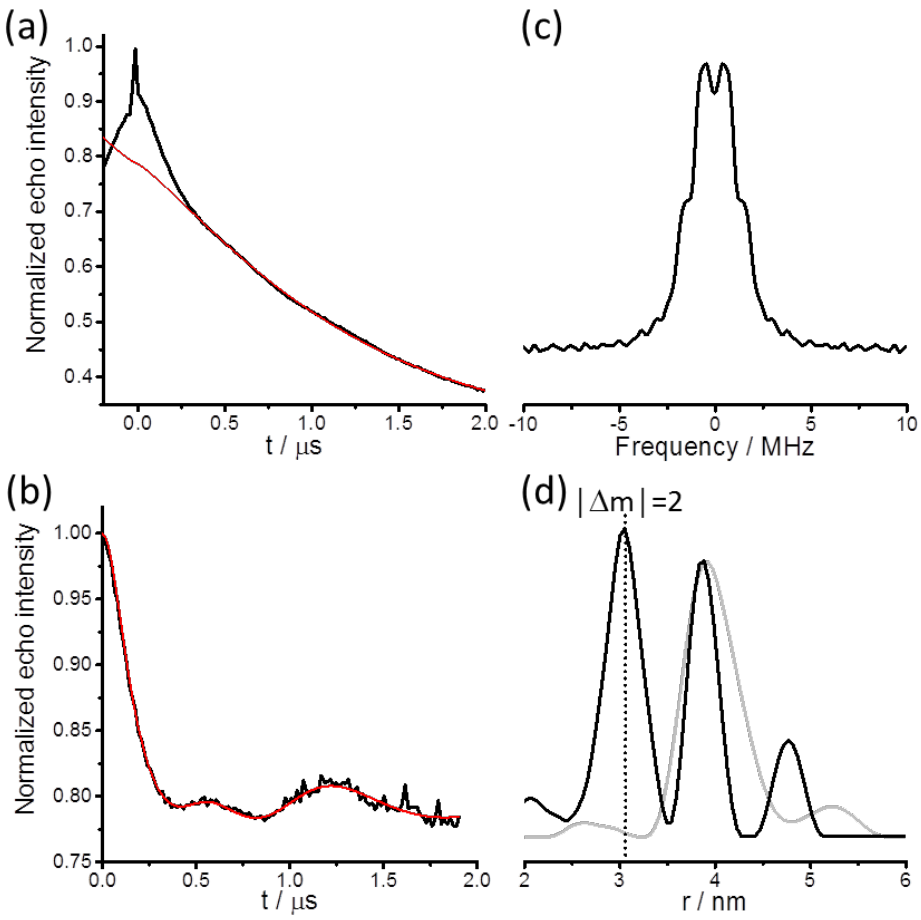

Figure S8. RIDME results of T4L-E-**T1**. (a) Primary data along with the background correction function used in red. (b) Background corrected RIDME trace (black) along with the fit obtained with the distance distribution shown in (d) (red). (c) Fourier transform of the experimental trace in (b). (d) Comparison of the distance distributions obtained from the analysis of RIDME (black) and DEER (grey) data. The dotted line shows the position expected for the second harmonic calculated from the main peak.

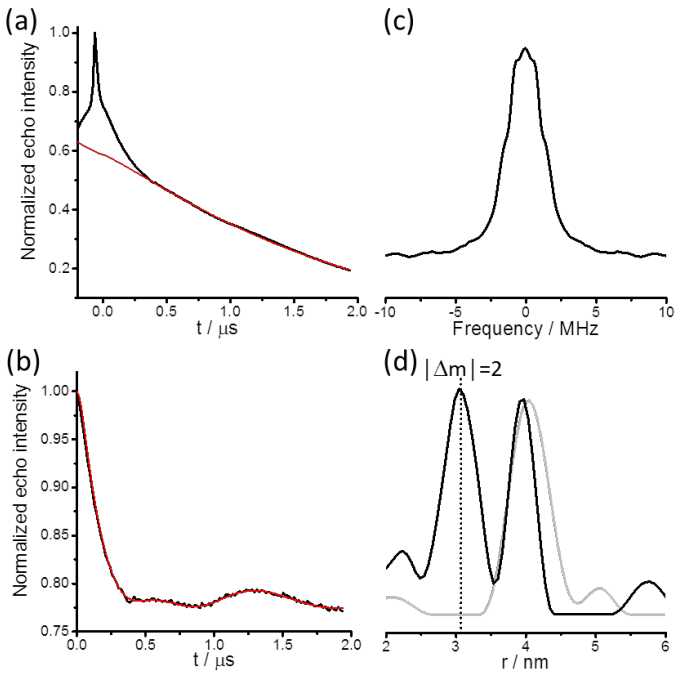

Figure S9. RIDME results of T4L-F-**T1**. (a) Primary data along with the background correction function used in red. (b) Background corrected RIDME trace (black) along with the fit obtained with the distance distribution shown on the right (red). (c) Fourier transform of the experimental trace in (b). (d) Comparison of the distance distributions obtained from the analysis of RIDME (black) and DEER (grey) data. The dotted line shows the position expected for the second harmonic calculated from the main peak.

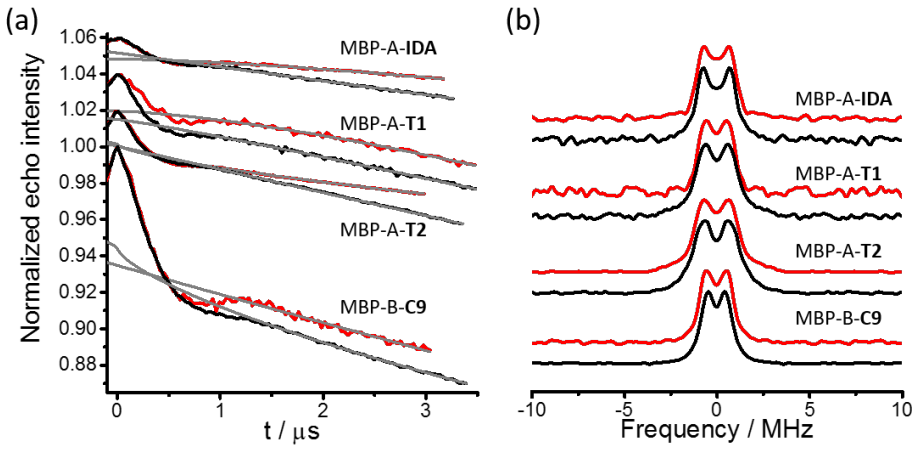

Figure S10. DEER data obtained with Gd^{3+} ions in different tags attached to MBP mutants in the presence (red) and absence (black) of one equivalent of maltose. (a) Primary DEER traces with background functions (grey). (b) Corresponding spectra after background subtraction and Fourier transformation.

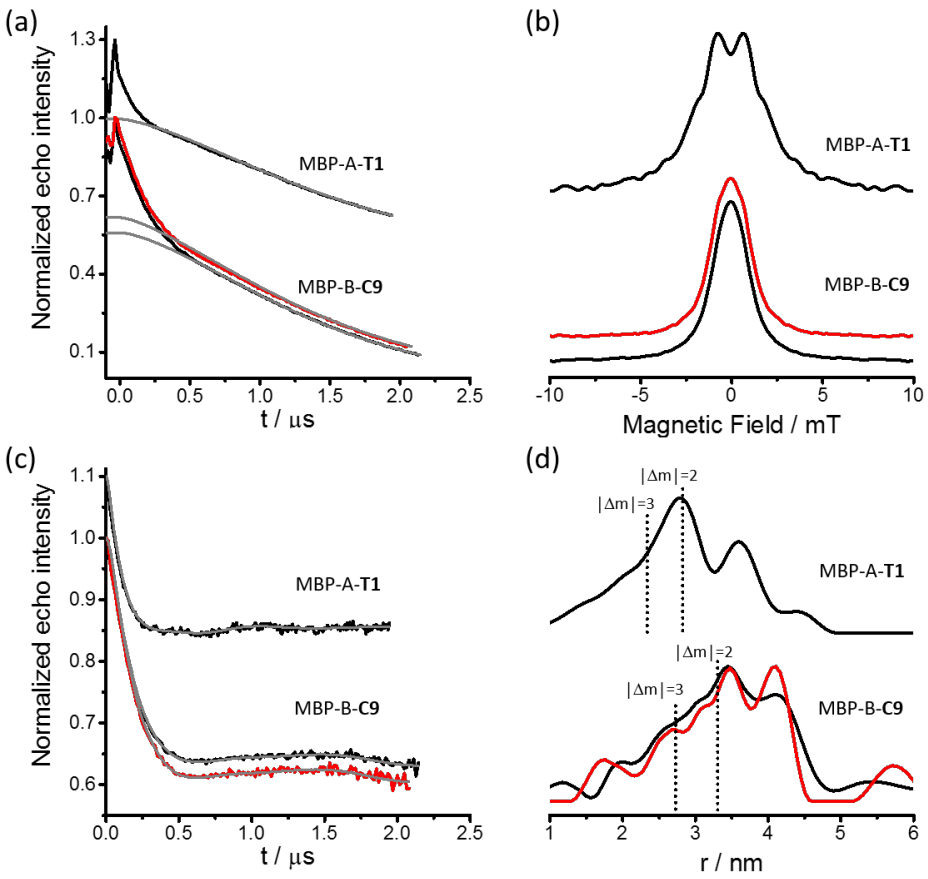

Figure S11. RIDME results obtained with MBP-A-**T1** and MBP-B-**C9** with (red) and without (black) one equivalent of maltose. (a) Primary RIDME traces. Grey lines indicate the background decay. (b) Corresponding spectra after background subtraction and Fourier transformation. (c) Background corrected RIDME traces. The grey lines correspond to the fits obtained with the distance distributions in (d). (d) Distance distributions obtained from data analysis. The dotted lines show the positions expected for the second and third harmonics calculated from the main peak.